Islamic University Journal of Applied Sciences (IUJAS)
https://journals.iu.edu.sa/jesc

Volume VIII, Issue I, July 2026, Pages 153-167

Numerical Vibration Analysis and Nonlinear Stability Prediction of Hydrodynamic Journal Bearings: Short and Long Bearing Configurations

Amira Amamou1[1,2], Amani Amamou [1,3], Nejla Mahjoub Said [4,*]

[1] Laboratory of Mechanical Engineering, National Engineering School of Monastir, University of Monastir, 5000 Monastir, Tunisia
[2]Faculty of Sciences of Monastir, University of Monastir, 5000 Monastir, Tunisia, amira.amamou@fsm.rnu.tn
[3] National Engineering School of Gasfa, University of Gafsa, 2112 Gafsa, Tunisia
amani.amamou@yahoo.fr
[4] Department of Physics, College of Science, King Khalid University, Abha, 61413, Saudi Arabia,

* Corresponding author: Nejla Mahjoub Said, *Email Address*: nalmahjoub@kku.edu.sa

Abstract

This study investigates a two-degree-of-freedom model of a rigid, symmetrical, and balanced rotor supported by two identical journal bearings. Hydrodynamic fluid forces are described using half Sommerfeld solutions combined with both short and long bearing approximations. Accurate prediction of stability boundaries and nonlinear behaviors near these limits, such as stable and unstable limit cycles, hysteresis, and jump phenomena, is essential for reliable rotor-bearing system design and operation. To achieve this, a continuation approach based on a predictor–corrector methodology is employed to trace equilibrium paths and bifurcation points. The results show that for short bearings (aspect ratio $D/L < 0.5$), a bearing parameter of 0.8 produces subcritical bifurcation at rotational speeds below the dimensionless threshold of 2.64. In contrast, for long bearings ($D/L > 1$), a parameter of 0.42 leads to supercritical bifurcation for speeds exceeding 1.67. These findings highlight the significant influence of bearing parameters and rotor dynamics on system stability and nonlinear response. Finally, numerical integration of the journal center motion validates the accuracy and robustness of the continuation-based predictions.

Keywords: Nonlinear stability; Rotor bearing system; Hopf bifurcation; Numerical integration; Numerical continuation.

https://doi.org/10.63070/jesc.2026.021
Received 24 December 2025; Revised 03 April 2026; Accepted 10 April 2026.
Available online 15 April 2026.
Published by Islamic University of Madinah on behalf of *Islamic University Journal of Applied Sciences*.
This is an open access article published under the Creative Commons Attribution 4.0 International license (CC BY 4.0):https://creativecommons.org/licenses/by/4.0/

1. Introduction

The stability of journal bearings is of utmost importance to ensure the safe operation of rotating machines. While modelling the rotor bearing system's dynamic characteristics, nonlinearities are induced due to self-excited vibrations caused by hydrodynamic bearing instability. Linear analysis is usually used to predict stability threshold speeds; the prediction is only valid for small motion about the equilibrium position. Nonlinear analysis, however, is required to predict rotor whirl motions which may cause rotors failure during operation.

Several authors have studied the dynamic behavior of journal bearings and how it affects rotor system vibration. Newkirk [1] reported on the self-excited instability motions of rotor bearings systems based on an experimental examination. He noticed that orbital motions appear at a frequency roughly equal to half the rotor speed. These findings were published in Hollis and Taylor [2]. In 1960, Holmes [3] estimated the oil whirl threshold speeds and then developed a stability chart for the rotor-bearing system considering oil film as elastic in a viscous system. Linear analysis of a rotor supported by hydrodynamic bearings has been also performed to forecast the instability threshold speed for the long bearing approximation model [4].

The investigation of the nonlinear effect on bearing stability indicated that either a supercritical or subcritical Hopf bifurcation indicates the beginning of instability. For supercritical behavior, a stable equilibrium solution of the equations of motion loses stability as the rotor speed increases, and a stable limit cycle emerges smoothly from the bifurcation point. However, unstable limit cycles appear at speeds below the stability threshold speed in a subcritical bifurcation point, creating the equilibrium point basin of attraction. Myers [5] used the Hopf bifurcation theory to forecast periodic orbits at rotor speeds near the critical stability speed of a long journal bearing. He discovered the existence of three distinct bifurcation areas in the parameter space of the steady-state eccentricity ratio. Related research for the short journal bearing was reported by Hollis and Taylor [2].

To analyze the stability of short journal bearings while taking the turbulence impact into consideration, Khonsari and Wang [6] applied the Hopf bifurcation theory. The analytical investigation of the stability of hydrodynamic journal bearings reported in several references [5-7] is restricted to predicting the Hopf bifurcation point, the kind of bifurcation, and the size and form of the limit cycles in the vicinity of the stability threshold speed. Several other foundational studies back up the results. In 1993, Childs [8] focused on rotordynamic stability analyses for fluid-film bearings. Ehrich [9], in 1992, reported subsynchronous whirl and hysteresis in experiments, characteristic of with subcritical Hopf bifurcation. San Andrés and Taylor [10] conducted experiments that validated nonlinear force interactions in rotor–bearing test rigs. Brockett and El-Sayed [11] analysed nonlinear transient

responses in journal-bearing systems focusing on the complex dynamic transitions caused by fluid-film forces. More recently, Tondl [12] along with Zhang and Meng [13] developed nonlinear models that describe nonlinear phenomena governing the transition from a stable equilibrium point to unstable limit cycles. Amamou [14] used numerical continuation and bifurcation analysis to predict the rotor safe operating speed range by determining an extended stability chart including the domain of the journal threshold stability speed and the boundaries of limit cycle bifurcations.

Tools for the continuation and bifurcation detection of equilibrium points and limit cycles of nonlinear ordinary differential equations have been extensively developed within the field of numerical continuation [15,16,17]. Classical continuation algorithms allow systematic tracing of solution branches and detecting qualitative changes such as saddle-node, pitchfork, and Hopf bifurcation, as well as the birth of periodic solutions. Among the early and influential developments are the software packages AUTO [18], CONTENT [19], and MATCONT [20], which provide robust algorithm for branch switching, Floquet multiplier computation, and stability analysis. Taken together, these tools form a powerful computational framework for understanding both local and global behaviours in nonlinear dynamical systems.

Building on our previous works [17], [21], in which the nonlinear analysis and stability of short and long hydrodynamic bearings were studied separately, the present work goes a step further by combining both short and long bearing configurations within a unified framework. This allows a direct comparison of their nonlinear dynamic behavior and bifurcation characteristics, revealing how bearing geometry, through the aspect ratio D/L, governs the transition between subcritical and supercritical regimes. In the present work, the stability analysis of a rigid and balanced rotor supported by hydrodynamic journal bearings is carried out using numerical continuation and verified by numerical integration. Both short and long models of a journal bearing under the half Sommerfeld boundary conditions are considered. The findings of the path following approach are supported by numerical simulation for a chosen set of bearing design parameters under specific working circumstances. This paper is organized as follows. First, a nonlinear dynamic model of a rotor bearing system with short and long journal bearing is introduced, expressed in terms of the nondimensional journal speed and bearing modulus. Next, numerical continuation techniques and bifurcation analyses of equilibrium points and limit cycles are presented to investigate the stability and bifurcation behavior of the rotor–bearing system. Finally, the main numerical results and findings of the present study are verified using numerical integration method focusing on the nonlinear response and stability characteristics of the investigated journal bearings.

2. Rotor bearing system modelling

The rotor, with a mass $2M$ is mounted in two symmetrical journal bearings. In Figure 1, O_j and O_b are respectively the journal center and the bearing center. The hydrodynamic forces $\boldsymbol{F}_\varepsilon$, $\boldsymbol{F}_\theta$ and constant load $\boldsymbol{W} = M\boldsymbol{g}$ are the external forces acting on the journal. The motion of the journal center is modeled through equations of motion written in terms of derivatives with respect to nondimensional time $\tau = \omega t$ are as follows:

$$\begin{aligned} \ddot{\varepsilon} - \varepsilon\dot{\theta}^2 &= \frac{-F_\varepsilon}{Mc\omega^2} + \frac{g}{c\omega^2}\cos\theta \\ \varepsilon\ddot{\theta} + 2\dot{\varepsilon}\dot{\theta} &= \frac{F_\theta}{Mc\omega^2} - \frac{g}{c\omega^2}\sin\theta \end{aligned} \tag{1}$$

ε and θ are respectively the eccentricity ratio and the attitude angle of the journal center. c is the radial bearing clearance and ω is the rotor rotating speed.

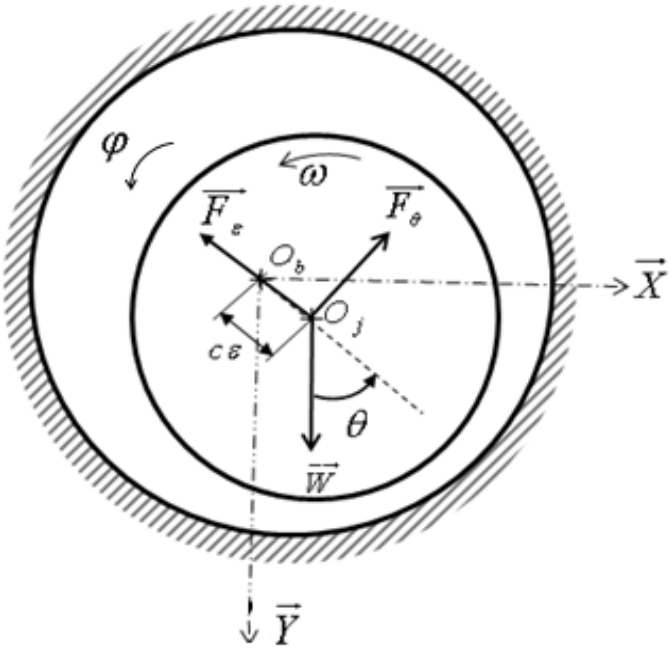


Figure 1. A hydrodynamic bearing cross section [17]

2.1 The short journal bearing model

Short bearings are commonly employed to minimize axial pressure variation and reduce frictional losses. Hydrodynamic force components in the rotating coordinates can be written as [2]:

$$\begin{cases} F_{\varepsilon} = \dfrac{\mu R L^3 \omega}{2c^2}\left[\dfrac{2\left(1-2\dot{\theta}\right)\varepsilon^2}{\left(1-\varepsilon^2\right)^2}+\dfrac{\pi\dot{\varepsilon}\left(1+2\varepsilon^2\right)}{\left(1-\varepsilon^2\right)^{2.5}}\right] \\ F_{\theta} = \dfrac{\mu R L^3 \omega}{2c^2\varepsilon}\left[\dfrac{\pi\left(1-2\dot{\theta}\right)\varepsilon^2}{2\left(1-\varepsilon^2\right)^{1.5}}+\dfrac{4\dot{\varepsilon}\varepsilon^2}{\left(1-\varepsilon^2\right)^2}\right] \end{cases} \tag{2}$$

where μ is the viscosity of the oil film, R is the journal radius and L is the bearing length.

Substituting the expressions of the hydrodynamic reactions (2) in the system of equations (1) and using the dimensionless bearing parameter $\Gamma = \dfrac{\mu R L^3}{2Mc^{2.5}g^{0.5}}$, the dimensionless journal speed $\varpi = \omega\sqrt{\dfrac{c}{g}}$ and the vector of state variables $\boldsymbol{X} = \begin{pmatrix} x_1 & x_2 & x_3 & x_4 \end{pmatrix}^T = \begin{pmatrix} \varepsilon & \theta & \dot{\varepsilon} & \dot{\theta} \end{pmatrix}^T$, the journal center equations of motion can be written in the following state space form:

$$\begin{cases} \dot{x}_1 = x_3 \\ \dot{x}_2 = x_4 \\ \dot{x}_3 = x_1 x_4^2 - \dfrac{\Gamma}{\varpi}\left[\dfrac{2\left(1-2x_4\right)x_1^2}{\left(1-x_1^2\right)^2}+\dfrac{\pi x_3\left(1+2x_1^2\right)}{\left(1-x_1^2\right)^{2.5}}\right] \\ +\dfrac{1}{\varpi^2}\cos\left(x_2\right) \\ \dot{x}_4 = \dfrac{-2x_3x_4}{x_1}+\dfrac{\Gamma}{\varpi}\left[\dfrac{\pi\left(1-2x_4\right)}{2\left(1-x_1^2\right)^{1.5}}+\dfrac{4x_3}{\left(1-x_1^2\right)^2}\right] \\ -\dfrac{1}{x_1\varpi^2}\sin\left(x_2\right) \end{cases} \tag{3}$$

For a given bearing parameter Γ, the system of equations (3) depends on ϖ and has the following form $\boldsymbol{X} = \boldsymbol{f}(\boldsymbol{X}, \varpi)$

2.2. The long journal bearing model

In the case of a long bearing, the axial flow can be neglected. The flow is then purely circumferential. The expressions of hydrodynamic force components are obtained as follows [21]:

$$\begin{cases} F_{\varepsilon} = \dfrac{6\mu LR^3\omega}{c^2}\left\{\dfrac{2\varepsilon^2\left(1-2\dot{\theta}\right)}{\left(2+\varepsilon^2\right)\left(1-\varepsilon^2\right)}+\dfrac{\left[\pi^2\left(2+\varepsilon^2\right)-16\right]\dot{\varepsilon}}{\pi\left(2+\varepsilon^2\right)\left(1-\varepsilon^2\right)^{1.5}}\right\} \\ F_{\theta} = \dfrac{6\mu LR^3\omega}{c^2}\left\{\dfrac{\pi\varepsilon\left(1-2\dot{\theta}\right)}{\left(2+\varepsilon^2\right)\left(1-\varepsilon^2\right)^{0.5}}+\dfrac{4\varepsilon\dot{\varepsilon}}{\left(2+\varepsilon^2\right)\left(1-\varepsilon^2\right)}\right\} \end{cases} \tag{4}$$

Using the nondimensional bearing parameter $\lambda = \dfrac{6\mu LR^3}{M\,c^{2.5}g^{0.5}}$ and $\varpi = \omega\sqrt{\dfrac{c}{g}}$, the dimensionless state space form $\boldsymbol{X} = \boldsymbol{f}(\boldsymbol{X},\varpi)$ that characterizes the development of the system state is $\boldsymbol{X} = \left(x_1 \quad x_2 \quad x_3 \quad x_4\right)^T = \left(\varepsilon \quad \theta \quad \dot{\varepsilon} \quad \dot{\theta}\right)^T$ produced and the following system of equations is obtained:

$$\begin{cases} \dot{x}_1 = x_3 \\ \dot{x}_2 = x_4 \\ \dot{x}_3 = x_1x_4^2 - \dfrac{\lambda}{\varpi}\left\{\dfrac{2x_1^2\left(1-2x_4\right)}{\left(1-x_1^2\right)\left(2+x_1^2\right)}+\dfrac{\left[\pi^2\left(2+x_1^2\right)-16\right]x_3}{\pi\left(2+x_1^2\right)\left(1-x_1^2\right)^{1.5}}\right\} \\ \quad +\dfrac{1}{\varpi^2}\cos\left(x_2\right) \\ \dot{x}_4 = \dfrac{-2x_3x_4}{x_1}+\dfrac{\lambda}{\varpi}\left\{\dfrac{\pi\left(1-2x_4\right)}{\left(2+x_1^2\right)\left(1-x_1^2\right)^{0.5}}+\dfrac{4x_3}{\left(2+x_1^2\right)\left(1-x_1^2\right)}\right\} \\ \quad -\dfrac{1}{x_1\varpi^2}\sin\left(x_2\right) \end{cases} \tag{5}$$

For a given bearing parameter λ and rotor speed ϖ, the nonlinear system of second order differential equations mentioned above may be solved.

3. Numerical continuation

It is necessary to have an initial steady state solution to use a continuation algorithm. For a given bearing parameter Γ and a nondimensional rotor speed ϖ, an equilibrium point for an autonomous nonlinear system of ordinary differential equations may be derived. This equilibrium point is unstable for a rotor speed greater than the stability threshold speed, and stable otherwise.

The numerical continuation is performed using the MatCont toolbox in MATLAB [20], which implements a predictor-corrector scheme. A tangent predictor generates an initial guess along the solution branch, with an initial step size of 0.1, adaptively adjusted within the range [10^{-5}, 0.5] based on the local behavior of the branch. The corrector phase relies on a pseudo-arclength Newton-Raphson

method, ensuring robust tracking of the solution branch including around turning points and bifurcations. Convergence is achieved when the residual norm satisfies $\|F(x)\| < 10^{-6}$, within a maximum of 10 Newton iterations per continuation step.

Subsequently, the branch of equilibrium points is found by numerical continuation using the rotor speed as a control parameter. The branch of limit cycles is then determined by continuation of limit cycles, starting from the Hopf bifurcation point. We are interested in finding possible bifurcations of limit cycles of the rigid rotor-bearing system for a selected value of the bearing parameter.

3.1 The short journal bearing: equilibrium point continuation and bifurcation detection

For a given bearing parameter Γ, numerical continuation extends the initial equilibrium point and tracks its path as the nondimensional rotating speed ϖ is varied where ϖ serves as the control parameter. When a Hopf bifurcation point 'H' is detected at $\varpi = \varpi_H = \varpi_c$, the first Lyapunov coefficient is automatically computed by MatCont. A negative Lyapunov coefficient indicates a supercritical Hopf bifurcation, in which stable limit cycles emerge from the bifurcation point for $\varpi \geq \varpi_H$. Conversely, a positive Lyapunov coefficient characterizes a subcritical Hopf bifurcation, where unstable limit cycles bifurcate from the Hopf point for $\varpi \leq \varpi_H$, potentially coexisting with the stable equilibrium and leading to more complex dynamic behavior.

As reported in [17], for short bearings, the value $\Gamma = 0.6$ acts as a transition threshold separating the two regimes: bearing parameters below this value give rise to supercritical behavior, while values above it lead to a subcritical behavior. To illustrate the subcritical regime, $\Gamma = 0.8$ is selected as a representative value, for which a subcritical Hopf bifurcation is observed at the threshold speed ϖ_H. Figure 2 illustrates the path of the initial equilibrium point obtained by numerical continuation, for the selected bearing parameter $\Gamma = 0.8$, as the nondimensional rotating speed ϖ is varied. The equilibrium curve reveals two distinct regions: the equilibrium point is stable for rotor speeds below the Hopf bifurcation point H, shown as a solid line, and becomes unstable beyond it, shown as a dashed line.

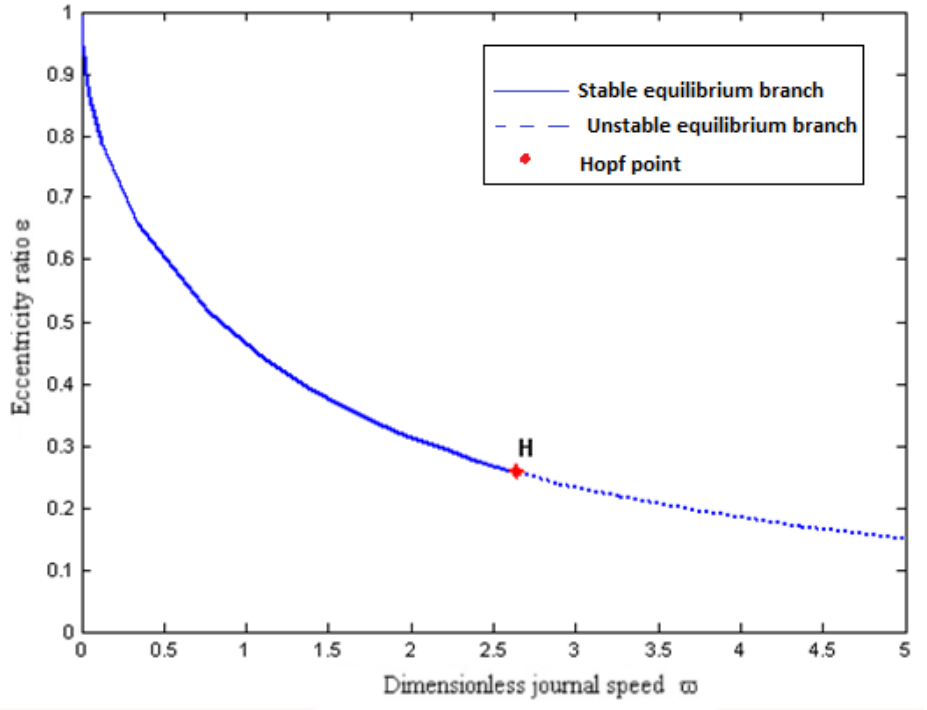


Figure 2: Equilibrium manifold in the (ϖ, ε) plane for a short journal bearing with bearing parameter $\Gamma = 0.8$

The Lyapunov coefficient for the Hopf point is equal to 1.86×10^{-2}. As a result, the Hopf point should give rise to an unstable limit cycle branch. The journal bearing behavior is then subcritical for rotational speeds below the threshold speed $\varpi < \varpi_c = 2.64$. The branch of limit cycles is determined by numerical continuation, which starts with the Hopf point and uses ϖ as a control parameter. Other bifurcations may also occur in limit cycles. For a rigid and balanced rotor, as long as the eccentricity limitations $\varepsilon = 1$ are not reached [15,22], limit cycles are only scheduled to cross a Limit Point of Cycles bifurcation (LPC).

At an LPC bifurcation point, stable and unstable periodic solution collide and disappear. An unstable limit cycle branch bifurcates from a stable limit cycle branch. The same thing happens when a branch of unstable limit cycles bifurcates into a branch of stable limit cycles. For the chosen bearing parameter $\Gamma = 0.8$, Only one bifurcation point has been found as seen in Figure 3.

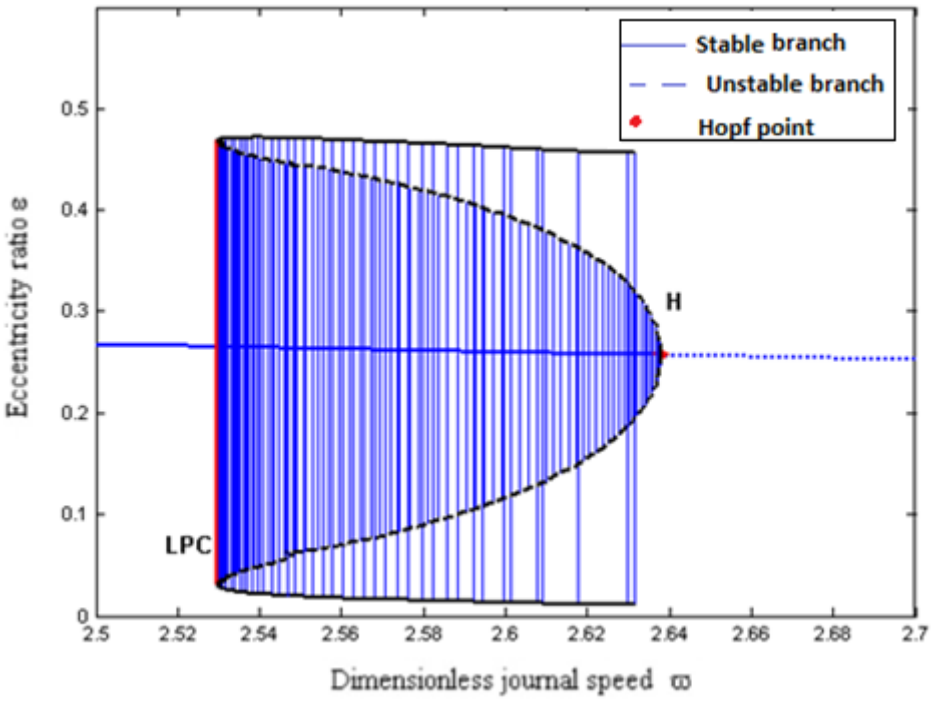


Figure 3: Subcritical limit cycle bifurcations for a bearing parameter $\Gamma = 0.8$

The unstable limit cycle in the range $\varpi_{LPC} < \varpi < \varpi_H$ defines the stable equilibrium solution's basin of attraction. The journal center returns to the stable equilibrium position if it is perturbed inside the basin of attraction. It diverges away from the basin of attraction to bigger stable limit cycles for greater disturbances, as seen in Figure 3.

For subcritical bifurcations, large unstable limit cycle exists until the saddle node (LPC) speed is reached. The ϖ_H and ϖ_{LPC} specify the rotor bearing system's hysteresis loop's boundaries. An unstable solution exists within the hysteresis loop. At a specific running speed, large disturbance exceeding the basin of stability causes the journal center to shift to large stable limit cycles, whereas disturbance within unstable orbit will decay to the equilibrium position.

The system of equations (3) for the short bearing model is numerically integrated to determine the journal center's trajectories to validate the predictions made by the numerical continuation approach. The pair (Γ, ϖ) must be chosen for the numerical simulation. Equations (3) are then integrated from the initial time up to a chosen end time, starting from a selected initial point $\left(\varepsilon_0 \quad \theta_0 \quad \dot{\varepsilon}_0 \quad \dot{\theta}_0\right)$ in the vicinity of the stability point.

The system tends to asymptotically approach the steady state equilibrium point for $\varpi = 2.54 < \varpi_c = 2.64$, if the journal center is released from a location inside the unstable periodic solution, in accordance with the properties of unstable periodic solutions. The initial positions are

shown with asterisk mark. Figure 4 depicts the locus of journal center that has been released from a position close to equilibrium point and has now settled to the steady state equilibrium point.

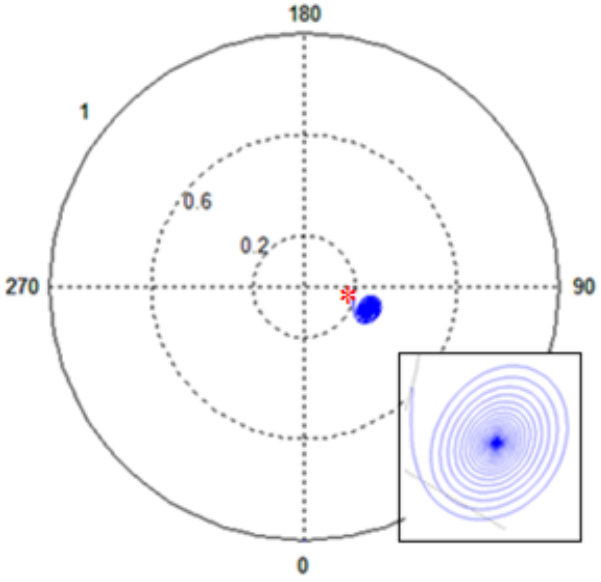


Figure 4: The journal center's trajectory deviated from its initial location inside the unstable limit cycle for $\Gamma = 0.8$ and $\varpi = 2.54$

The shaft is moving at the same speed $\varpi = 2.54$ during the second simulation, but it is let go from a starting position that is outside the unstable limit cycle. As shown in Figure 5, the rotor bearing system, in this instance, converges to a stable limit cycle.

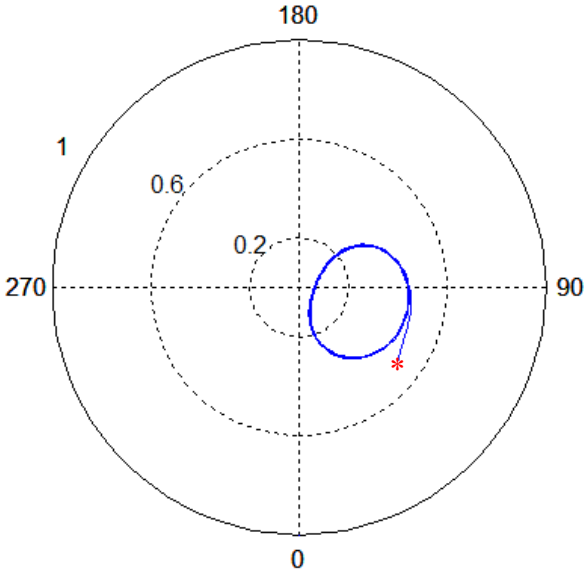


Figure 5: The journal center's trajectory deviated from a point outside the unstable limit cycle for $\Gamma = 0.8$ and $\varpi = 2.54$

3.2 The long journal bearing: equilibrium point continuation and bifurcation detection

The one parameter bifurcation analysis of equilibrium points and the detection of their bifurcations for the rotor bearing system with a journal bearing parameter $\lambda = 0.42$ is carried out. As reported in [5, 22], the bifurcation is subcritical for $\lambda \leq 0.27$ and $\lambda \geq 4.43$, and supercritical for $0.27 < \lambda < 4.43$. Accordingly, a bearing parameter $\lambda = 0.42$ is selected as a representative value within the supercritical range, for which a stable supercritical behavior is predicted.

The one parameter bifurcation analysis of equilibrium points and the detection of their bifurcations for the rotor bearing system with a journal parameter $\lambda = 0.42$ is carried out. A stable supercritical behavior is predicted, as reported in work [5, 22], for running speeds $\varpi > \varpi_c = 1.67$. A trajectory that converges with the steady state equilibrium position represents a behavior at a stable point. Beyond a supercritical bifurcation, the trajectories of the journal center must converge to a periodic limit cycle at beginning positions within or outside the limit cycle envelope for speeds higher than the critical stability speed ϖ_c. By numerical continuation, an equilibrium point is located and then continued with respect to the journal speed ϖ which represents the continuation parameter to define the path of the equilibrium point as shown in Figure 6.

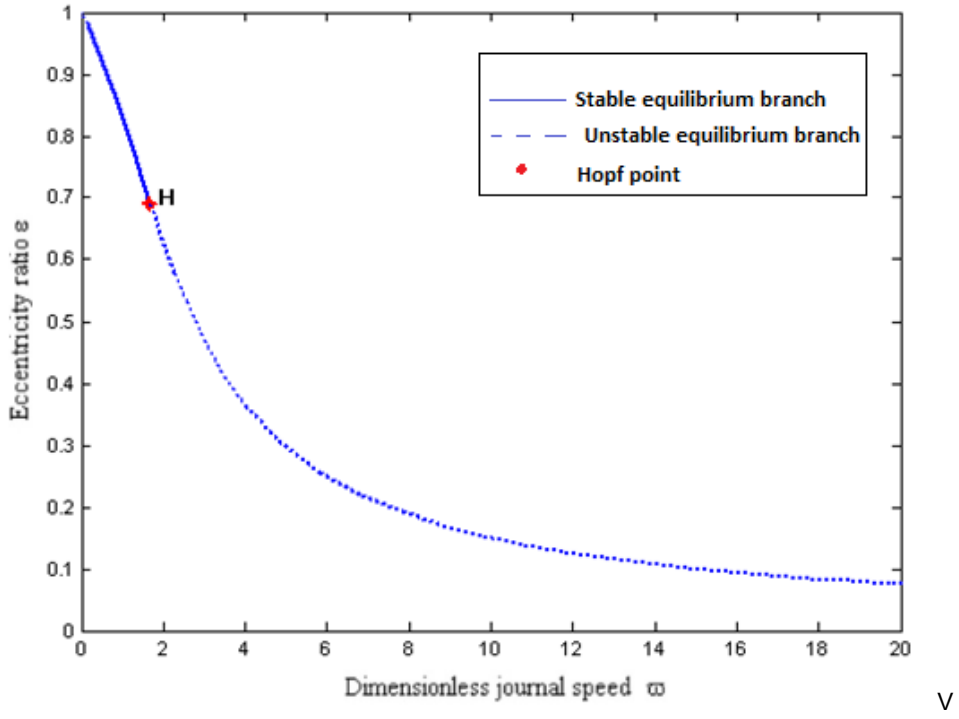


Figure 6: Equilibrium manifold in the (ϖ, ε) plane for a long journal bearing with bearing parameter $\lambda = 0.42$

Lyapunov coefficient is equal to -3.24×10^{-1} at $\varpi = \varpi_H = 1.67$, indicating a supercritical Hopf bifurcation since it is negative. Once a Hopf bifurcation is detected, numerical continuation of limit cycles is applied to determine the branch of stable limit cycles as shown in Figure 7.

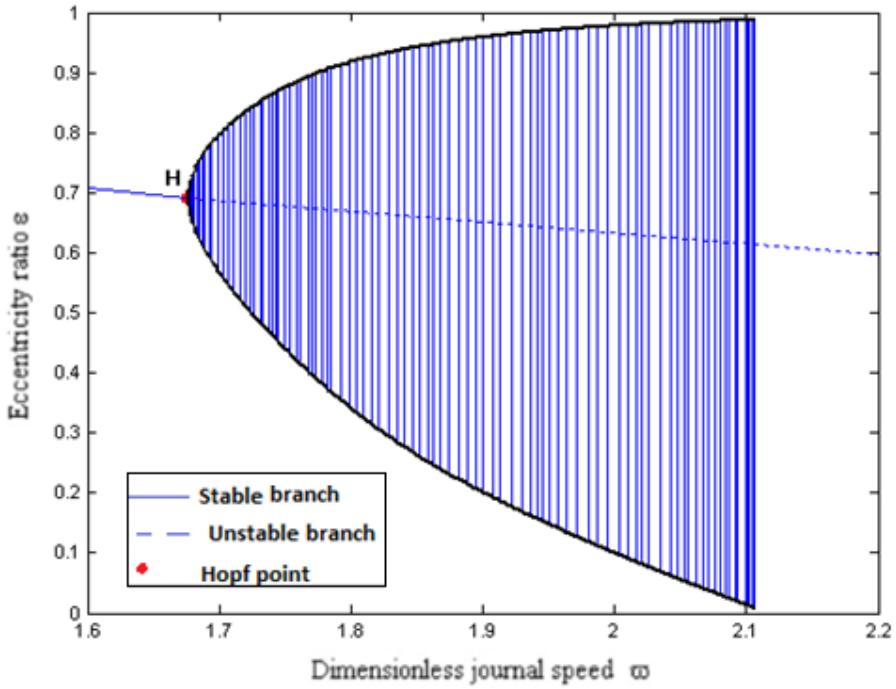


Figure 7: The branch of stable limit cycles bifurcating from the Hopf point H for a bearing parameter $\lambda = 4.2$

The stable limit cycle branch in Figure 7 has been extended until the clearance limit is reached. No LPC bifurcation is detected for the supercritical limit cycles before reaching the clearance limit. Increasing the running speed ϖ, the size of the limit cycles grows gradually with the running speed ϖ. Figure 7 reveals that the periodic solutions may be of high amplitude and involve contact with the bearing's housing.

Notably, a low amplitude limit cycle appears directly as the rotor speed exceeds the threshold speed. A numerical simulation is carried out to verify the above results and to investigate how the whirl orbits develop at rotor speeds away from the threshold speed.

Figures 8 (a) and 8 (b) show the existence of stable limit cycles for dimensionless speed $\varpi = 2 > \varpi_c = 1.67$.

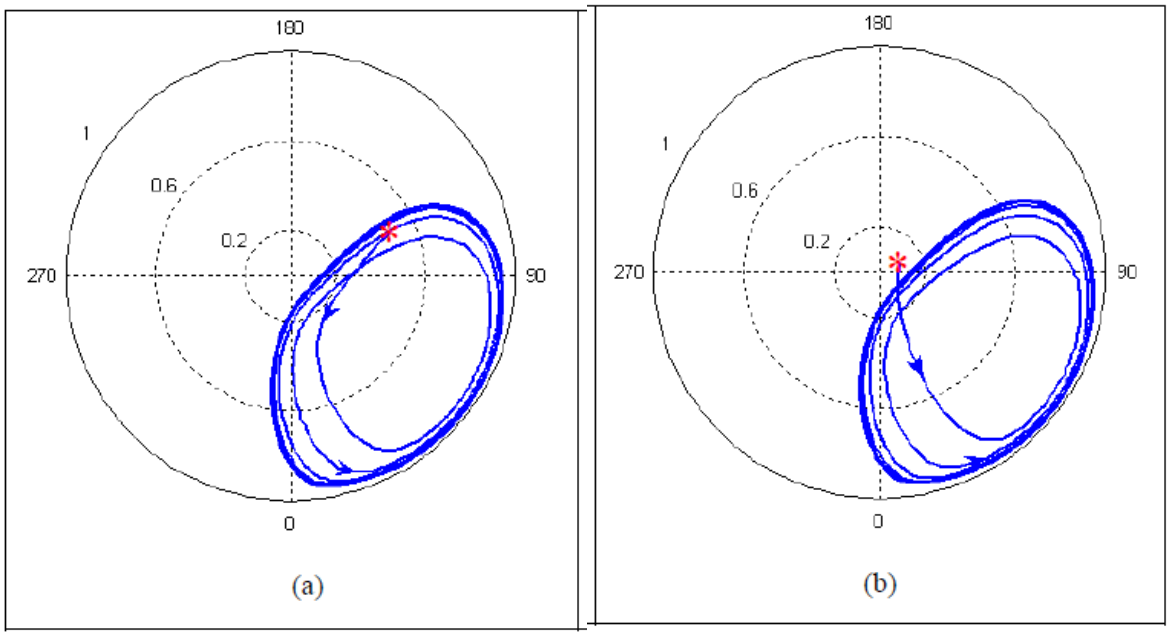


Figure 8: Phase plane trajectories of the journal center for $\lambda = 0.42, \varpi = 2$: (a) initial point in the stable region, (b) initial point outside the stable region

It can be noted that the trajectories of journal center converge to the same limit cycle whether the initial point is chosen inside the limit cycle envelope, Figure 8 (a), or outside the limit cycle envelope, Figure 8 (b).

4. Conclusion

A comprehensive nonlinear analysis of stability and bifurcation behaviors is presented for a perfectly balanced rigid rotor supported by identical hydrodynamic journal bearings using numerical continuation via the MatCont toolbox. Both short and long bearing models, formulated under the half-Sommerfeld boundary conditions, are considered, allowing a broad and realistic representation of bearing configurations.

The study reveals fundamentally different dynamic behaviors depending on key design parameters such as rotational speed, applied load, the bearings lubrication characteristics, and the bearing geometry, as characterized by the aspect ratio D/L. Indeed, Hopf bifurcations may be either subcritical or supercritical. As reported in [17], for the short bearing (D/L < 0.5), the bifurcation is subcritical for $\Gamma \geq 0.6$ and supercritical for $\Gamma < 0.6$, while for the long bearing (D/L > 1), the bifurcation is subcritical for $\lambda \leq 0.27$ and $\lambda \geq 4.43$, and supercritical for $0.27 < \lambda < 4.43$ as demonstrated in [5,22].

To illustrate these contrasting behaviors, two representative cases are examined. For the short bearing with $\Gamma = 0.8$, a subcritical Hopf bifurcation is observed at the threshold speed $\varpi_H = 2.64$, giving rise

to unstable limit cycles below this speed and indicating an abrupt and potentially dangerous loss of stability. In contrast, for the long bearing with $\lambda = 0.42$, a supercritical Hopf bifurcation occurs at the threshold speed $\varpi_H = 1.67$, producing stable limit cycles beyond this speed and reflecting a safer and more predictable dynamic transition. The short bearing reaches instability at a higher threshold speed but in a more abrupt and dangerous manner, while the long bearing loses stability earlier but more gradually. These two cases clearly highlight how the aspect ratio D/L, together with the bearing parameter, governs the nature of the bifurcation and consequently the safety of the rotor bearing system.

Numerical continuation of the limit cycles emanating from the Hopf bifurcation points, together with the detection of limit point of cycles (LPC) bifurcations, enables an accurate delineation of the system's stability boundaries and the identification of operating regions prone to hysteresis phenomena. A detailed numerical investigation corroborates the results obtained through continuation methods, confirming the validity and robustness of the proposed approach.

The findings of this work provide valuable guidelines for selecting appropriate system parameters to prevent undesirable journal center trajectories and self-excited vibrations, thereby enhancing the operational reliability, durability, and overall service life of rotor bearing systems. Future work will focus on extending this analysis to more complex configurations, including floating ring and tilting-pad bearings, and on investigating the influence of thermal effects, bearing misalignment, and shaft flexibility on the predicted bifurcation thresholds.

Funding

The authors declare that this research received no external funding.

Data Availability Statement

Not applicable.

Conflicts of Interest

The authors declare no conflict of interest.

References

[1] B. L. Newkirk, Shaft Whipping due to Oil Action in Journal Bearings, G.E. Rev. 27(1924) 169-178.

[2] P. Hollis, D. Taylor, Hopf Bifurcation to Limit Cycles in Fluid Film Bearings. J. Tribol. Trans. ASME. 108(1998) 184-189.

[3] R. Holmes, The Vibration of a Rigid Shaft on Short Sleeve Bearings, J. Mech. Eng. Sci. 2 (1960) 337-341.

[4] M.M. Reddi, P.R. Trumpler, Stability of the high-speed journal bearing under steady load, ASME J. Eng. Ind. 84 (1962) 351–358.

[5] C. J. Myers, Bifurcation theory applied to oil whirl in plain cylindrical journal bearings, J. Appl. Mech. Trans. ASME. 51(1984) 244-250.
[6] J. K. Wang, M. M. Khonsari, Application of Hopf bifurcation theory to rotor-bearing systems with consideration of turbulent effects, J. Tribol.Int.39(7) (2006) 701- 714.
[7] J. W. Lund, Oil Whip Whirl Orbit of a Rotor in Sleeve Bearings, ASME J. Eng. Ind. 89 (1967) 813-823.
[8] D. W. Childs, Turbomachinery Rotordynamics: Phenomena, Modeling, and Analysis.
Wiley, New York,1993.
[9] F.F. Ehrich, Handbook of Rotordynamics, McGraw-Hill, New York,1992.
[10] L. San Andrés, C. F. Taylor, Experimental identification of nonlinear rotordynamic coefficients in fluid-film bearings, J. Tribol.Trans. ASME. 118 (1996) 39–47.
[11] R. W. Brockett, A. El-Sayed, Nonlinear transient response of journal-bearing supported rotors. J. Sound Vib. 201(1) (1997) 1–15.
[12] A. Tondl, To the problem of self-excited vibrations in rotating machinery.Eng.Mech**.**7(1) (2000) 1–15.
[13] H. Zhang, G. Meng, Nonlinear dynamic modeling of rotor–bearing systems with fluid-film forces. J. Sound Vib. 273 (2004) 175–193.
[14] A. Amamou, Nonlinear stability analysis and numerical continuation of bifurcations of a rotor supported by floating ring bearings. Proc. IMechE Part C: J. Mech. Eng. Sci. 236 (2021) 1-13.
[15] Yu. A. Kuznetsov, Elements of Applied Bifurcation Theory, Springer-Verlag, 1998.
[16] B. Krauskopf, Numerical continuation methods for dynamical systems: path following and boundary value problem, Springer,2007.
[17] M. Chouchane, A. Amamou, Bifurcation of Limit Cycles in Fluid Film Bearings, Int. J. Non-Linear Mech.46 (2011) 1258-1264.
[18] E. J. Doedel et al., AUTO-07P: Continuation and Bifurcation Software for Ordinary Differential Equations (manual), January 2012
[19] Yu. A. Kuznetsov, H. G. E. Meijer, Numerical Bifurcation Analysis of Maps, Cambridge University Press, New York,2019.
[20] A. Dhooge, W. Govaerts, and Yu. A. Kuznetsov, MATCONT: A MATLAB package for continuation and bifurcation analysis, ACM Trans. Math. Softw. 29 (2003) 141 - 164.
[21] J. Frene, et al., Hydrodynamic Lubrication Bearings and Thrust Bearings, Elsevier, Tribology Series, Amsterdam,1997.
[22] A. Amamou, M. Chouchane, Nonlinear stability analysis of long hydrodynamic journal bearings using numerical continuation, Mech. Mach. Theory. 72 (2014) 17-24.